Applied Catalysis B: Environmental 275 (2020) 119105

Contents lists available at ScienceDirect

Applied Catalysis B: Environmental

journal homepage: www.elsevier.com/locate/apcatb

Hydrothermal aging alleviates the inhibition effects of NO_2 on Cu-SSZ-13 for NH_3-SCR

Yulong Shan[a], Yu Sun[a,c], Jinpeng Du[a,c], Yan Zhang[b], Xiaoyan Shi[a,c], Yunbo Yu[a,b,c], Wenpo Shan[b,*], Hong He[a,b,c]

[a] State Key Joint Laboratory of Environment Simulation and Pollution Control, Research Center for Eco-Environmental Sciences, Chinese Academy of Sciences, Beijing 100085, China

[b] Center for Excellence in Regional Atmospheric Environment, Institute of Urban Environment, Chinese Academy of Sciences, Xiamen 361021, China

[c] University of Chinese Academy of Sciences, Beijing 100049, China

ARTICLE INFO

Keywords:
Hydrothermal aging
Fast SCR
Inhibition effects
Cu-SSZ-13
Brønsted acid sites

ABSTRACT

Fresh and hydrothermally aged Cu-SSZ-13 catalysts were tested for the standard and fast selective catalytic reduction of NO_x with NH_3 (NH_3-SCR). Interestingly, NO_2 exhibited distinctly different effects on these two catalysts. NO_x conversion over fresh Cu-SSZ-13 was clearly inhibited by NO_2, while hydrothermal aging could reverse this inhibition effect. It was found that the NO_x conversion decreased with progressive hydrothermal aging under standard SCR (SSCR) conditions but increased under fast SCR (FSCR) conditions. The N_2 adsorption/desorption isotherms indicated the formation of mesopores induced by hydrothermal aging, which is favorable for gas diffusion. Temperature programmed desorption (TPD) and *in situ* DRIFTS, combined with other auxiliary measurements, demonstrated that L-NH_3 (NH_3 adsorbed onto Lewis acid sites) is more active toward both NO + O_2 and NO_2 for the formation of N_2, while B-NH_3 (NH_3 adsorbed onto Brønsted acid sites) is mainly responsible for the formation of NH_4NO_3. The amount and stability of NH_4NO_3 formed under FSCR conditions decreased with progressive hydrothermal aging due to the loss of Brønsted acid sites.

1. Introduction

NO_x in the atmosphere play critical roles in the emergence of severe air pollution problems, such as acid rain, photochemical smog, and haze. [1] Diesel vehicles are important sources for NO_x emissions. Selective catalytic reduction of NO_x with NH_3 (NH_3-SCR) is the dominant technology for the abatement of NO_x from lean-burn diesel engines. Although great efforts have been devoted to the development of NH_3-SCR catalysts in the last few decades, great challenges remain in meeting the ever-tightening emission standards. One of the biggest challenges is hydrothermal aging, because NH_3-SCR catalysts are exposed to high temperature and humid conditions during the regeneration of the diesel particulate filter (DPF). [2] In the last decade, the consensus of the NH_3-SCR catalysis community for diesel vehicles has changed significantly. Typically, the Cu-exchanged small-pore SSZ-13 zeolite has replaced traditional vanadium-based oxides and Fe-ZSM-5/Fe-Beta catalysts to become the current standard commercialized NH_3-SCR catalyst due to its outstanding deNO_x activity and hydrothermal stability. [3,4]

The hydrothermal aging mechanism of Cu-SSZ-13 zeolites has been extensively investigated in previous studies. [5–13] In summary, hydrothermal aging will induce loss of active sites and destruction of the zeolite skeleton structure, thus resulting in the deactivation of Cu-SSZ-13 catalysts. However, knowledge on the properties and catalytic performance of hydrothermally aged Cu-SSZ-13 is still incomplete. For example, the effects of co-existing SO_2, NO_2, or HCs on hydrothermally aged Cu-SSZ-13 have been little studied. The investigation of these effects is very meaningful in practical terms, because the actually applied NH_3-SCR catalysts are always in a hydrothermally aged state. Our group previously investigated the deactivation of Cu-SSZ-13 in the presence of SO_2 during hydrothermal aging, and found that more severe degradation of the zeolite structure occurred compared with Cu-SSZ-13 subjected to hydrothermal aging alone. [14] Wei et al. investigated the impact of hydrothermal aging on the SO_2 poisoning of Cu-SSZ-13 catalysts. They found that a mildly hydrothermally aged Cu-SSZ-13 catalyst showed higher SO_2 tolerance than fresh and severely hydrothermally aged ones due to its more facile desulfation. [15] In addition to SO_2, the effects of other important co-existing gases on hydrothermally aged Cu-SSZ-13 catalyst still need to be explored.

The effects of co-existing NO_2 in actual diesel exhaust is important

* Corresponding author.
E-mail address: wenposhan@hotmail.com (W. Shan).

https://doi.org/10.1016/j.apcatb.2020.119105
Received 1 March 2020; Received in revised form 30 April 2020; Accepted 5 May 2020
Available online 08 May 2020

because it can participate in NO_x reduction through the so-called "fast SCR" reaction (reaction 1), in addition to the standard SCR reaction (reaction 2) [16–20].

$$\text{Fast SCR:}2NH_3 + NO + NO_2 \rightarrow 2N_2 + 3H_2O \quad (1)$$

$$\text{Standard SCR:}4NH_3 + 4NO + O_2 \rightarrow 4N_2 + 6H_2O \quad (2)$$

In general, the deNO_x efficiency of SCR catalysts will significantly increase for NH_3-SCR catalysts when NO_2 is introduced to the reaction atmosphere due to the occurrence of the fast SCR reaction [21–23]. However, Kwak et al. found that their Cu-SSZ-13 catalyst (with Si/Al of ~6) showed only a slight improvement in NO_x conversion under fast SCR conditions [24]. Afterwards, our group found that the addition of NO_2 even significantly inhibited the reduction of NO due to NH_4NO accumulation, and the inhibition effects closely correlated with the Cu loadings of Cu-SSZ-13 catalysts (with Si/Al of ~4.5) [25,26]. Moreover, we found that the fast SCR reaction was actually inhibited at low temperatures, while it occurred at high temperatures even on H-SSZ-13 zeolite [26]. Nevertheless, the effects of NO_2 on the hydrothermally aged Cu-SSZ-13 catalyst are still lacking, despite its practical significance, and the location for NH_4NO_3 formation is still under debate.

This study aimed to reveal the effect of NO_2 on the hydrothermally aged Cu-SSZ-13 catalyst and its comparison with the behavior of the fresh Cu-SSZ-13 catalyst. In addition, through the adjustment of active Cu^{2+} sites and acid sites by hydrothermal aging, the significance of NH_4NO_3 formation and its impact on the SCR reaction are discussed. Temperature programmed desorption (TPD) and *in situ* diffuse reflectance infrared Fourier transform spectroscopy (*in situ* DRIFTS), along with other auxiliary measurements, were employed to achieve these goals.

2. Experimental section

2.1. Catalyst synthesis

The initial Cu-SSZ-13 zeolite was synthesized in-situ by a one-pot method. [27] The initial Cu-SSZ-13 zeolite was post-treated with 0.1 mol/L HNO_3 at 80 °C for 12 h prior to filtration, washing and calcination at 600 °C for 6 h. Then, the obtained Cu-SSZ-13 catalyst was stirred in 0.01 mol/L NH_4NO_3 solution at 40 °C for 5 h for the second post-treatment process, followed by filtration, washing and calcination at 600 °C for 6 h. The obtained Cu-SSZ-13 catalyst had a Cu loading of ~3.8 wt.% (594 μmol/g), with Cu/Al and Si/Al of 0.3 and 4.5, respectively.

In addition, the Cu-SSZ-13 catalyst was hydrothermally aged in 10 vol.% H_2O/air at 750 °C for 16 h and 800 °C for 5 h, with the products denoted as Cu-SSZ-13 − 750 and Cu-SSZ-13 − 800, respectively.

2.2. Catalyst evaluation

The NH_3-SCR reaction measurements were conducted in a fixed-bed flow reactor system with an online Nicolet IS10 spectrometer, which was used to analyze the concentrations of NO, NO_2, N_2O, and NH_3. The reaction conditions were 500 ppm NO for standard SCR (SSCR) or 250 ppm NO + 250 ppm NO_2 for fast SCR (FSCR), 500 ppm NH_3, 5% O_2, 5 vol.% H_2O and balance N_2, with a total flow rate of 500 mL/min. About 50 mg catalyst was used for NH_3-SCR evaluation, with a gas hourly space velocity (GHSV) of ~ 400,000 h^{-1}. The NO, NO_2, and NO_x conversion percentages were calculated based on the inlet and outlet concentrations at steady state:

$$\text{NO conversion}= \left(1 - \frac{[NO]_{out}}{[NO]_{in}}\right) \times 100\%$$

$$NO_2 \text{ conversion}= \left(1 - \frac{[NO_2]_{out}}{[NO_2]_{in}}\right) \times 100\%$$

$$NO_x \text{ conversion}= \left(1 - \frac{[NO]_{out} + [NO_2]_{out}}{[NO]_{in} + [NO_2]_{in}}\right) \times 100\%$$

2.3. Catalyst characterization

Inductively coupled plasma Atomic Emission Spectroscopy (ICP-AES) was used to measure the elemental composition of the catalysts. Powder X-ray diffraction (PXRD) analysis was conducted on a computerized Bruker D8 Advance diffractometer with Cu Kα (λ = 0.15406 nm) radiation at room temperature, and the data were collected with 2θ ranging from 5° to 40° and step size of 0.02°. Solid state ^{27}Al MAS NMR spectra were collected on a Bruker AVANCE III 400 WB spectrometer using a 4 mm standard bore CP MAS probe. A physisorption analyzer (Micromeritics ASAP 2020 M and Tristar system) was used to measure pore structure (volume and size) of the samples by N_2 adsorption-desorption at 77 K. All samples were degassed at 90 °C for 12 h to remove the physisorbed moisture before N_2 adsorption.

Temperature-programmed reduction by H_2 (H_2-TPR) was carried out using a Micromeritics AutoChem 2920 chemisorption analyzer to identify copper species in the Cu-SSZ-13 catalysts. A 50 mg sample was put into a U-type tube and pretreated in 20 % O_2/N_2 at 500 °C for 40 min. After cooling down to 50 °C, O_2/N_2 was turned off and 10 % H_2/Ar was introduced, followed by ramping the temperature to 1000 °C at a rate of 10 °C/min. Temperature-programmed desorption was performed after the fast SCR reaction (FSCR-TPD) to identify the surface species of Cu-SSZ-13 after the FSCR reaction. The FSCR was carried out first at 200 °C, and the flow was switched to N_2 only and the temperature was decreased to 50 °C. After purging for 60 min, the temperature was increased to 700 °C with a rate of 10 °C/min, and the desorption of NO, NO_2, N_2O, and NH_3 was detected. Temperature-programmed desorption experiments with NH_3 (NH_3-TPD) and NO_x (NO_x-TPD) were conducted, respectively, using the NH_3-SCR activity measurement instrument. In this case, the Cu-SSZ-13 catalyst was first pretreated in 5% O_2/N_2 at 500 °C for 30 min. After cooling down to 50 °C, 5% O_2/N_2 was turned off and the sample was exposed to 500 ppm of NH_3 or NO_x for 1 h, followed by N_2 purging for 1 h. Finally, the temperature was raised to 600 °C in N_2 at the rate of 10 °C/min.

The in-situ DRIFTS experiments were performed using an FTIR spectrometer (Nicolet IS10) equipped with a Smart Collector and MCT/A detector. An Omega Programmable Temperature Controller was used to regulate the reaction temperature. Prior to each experiment, the catalyst was pretreated at 500 °C for 30 min in a flow of 20 % O_2/N_2 and then cooled down to 200 °C. The background spectrum was collected in flowing N_2 and automatically subtracted from the sample spectrum. The sample spectra from 4000 to 600 cm^{-1} were collected when the catalyst was exposed to the dry SSCR and FSCR reaction atmospheres. To investigate the transient processes of the SSCR and FSCR reactions, the sample was first exposed to a flow of 500 ppm NH_3/N_2 at 200 °C for 1 h, followed by N_2 purge for another 1 h. Afterwards, 500 ppm NO/N_2 + 5% O_2/N_2 and 500 ppm NO_2/N_2 were introduced to the flow to react with the adsorbed NH_3 species. All spectra were recorded by accumulating 100 scans with a resolution of 4 cm^{-1}.

3. Results and discussion

3.1. Physicochemical properties

The copper active sites and zeolitic structure of the obtained fresh and hydrothermally aged Cu-SSZ-13 catalysts were analyzed by H_2-TPR, XRD, and ^{27}Al-NMR, and the results are shown in Fig. 1**a**. The deconvolution of H_2-TPR profiles and the calculated amounts of Cu species, using the reduction of CuO for calibration, are shown in Fig. S1 and Table 1, respectively. The fresh Cu-SSZ-13 catalyst showed no CuO_x-related peak, but two prominent peaks at 230 and 320 °C, ascribed to $[Cu(OH)]^+$-Z and Cu^{2+}-2Z species, respectively. [9,28–30]

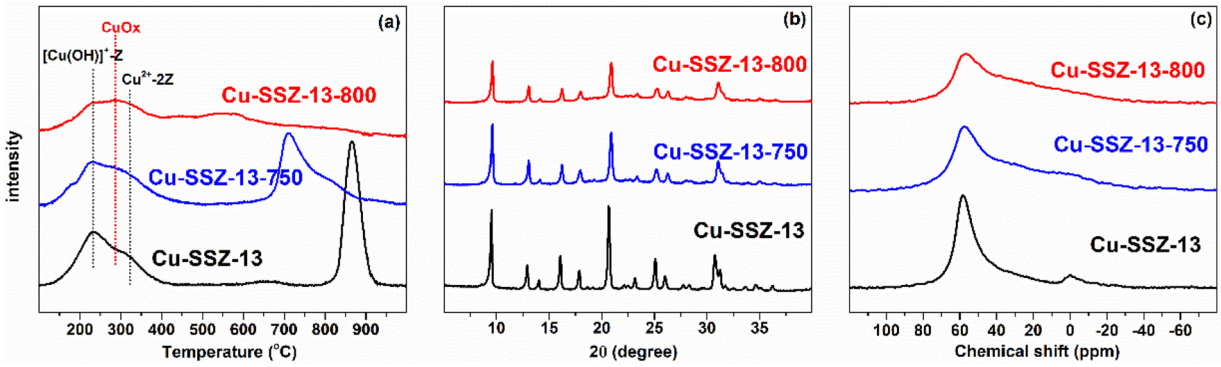

Fig. 1. Characterization results of fresh and hydrothermally aged Cu-SSZ-13 catalysts. (a) H_2-TPR profiles; (b) XRD patterns; (c) ^{27}Al-NMR profiles.

The peak at 880 °C was attributed to the reduction of Cu^+ to Cu°. [31,32] After hydrothermal aging at 750 °C, the conversion of $[Cu(OH)]^+$-Z to CuO_x was observed as previously reported. [8] The 800 °C hydrothermally aged Cu-SSZ-13 showed more CuO_x formation. With the increase of the hydrothermal aging temperature, the reduction temperature of Cu^+ to Cu° shifted to lower temperature, which indicated that the Cu^+ species was less stable. In addition, Table 1 shows that the total Cu amount (569 and 562 μmol/g) determined by H_2-TPR is approximately equal to the Cu loading (594 μmol/g) determined by ICP for the Cu-SSZ-13 and Cu-SSZ-13 – 750 samples. However, the Cu-SSZ-13 – 800 sample, after deep hydrothermal aging, showed a considerable decrease in the amount of Cu (346 μmol/g) determined by H_2-TPR, compared to 594 μmol/g by ICP, probably due to the formation of a Cu-aluminate-like phase, which is difficult to identify by H_2-TPR at low temperatures. [33–35]

XRD and ^{27}Al-NMR measurements were carried out to analyze the degradation of the zeolite structure caused by hydrothermal aging, and the results are shown in Fig. 1**b** and **1c**, respectively. Although the Cu-SSZ-13 – 750 and Cu-SSZ-13 – 800 samples showed a marked decrease in intensity for the typical CHA diffraction peaks, their CHA framework structures were still maintained (Fig. 1b). As shown in their ^{27}Al-NMR profiles (Fig. 1c), both of the hydrothermally aged Cu-SSZ-13 catalysts showed a decrease in framework Al (58 ppm), accompanied by the appearance of extra-framework Al (33 and 0 ppm) [36,37], indicating the occurrence of dealumination. The N_2 adsorption/desorption isotherms were also measured, with the results shown in Fig. S2, which showed the characteristic signature of microporous materials. The micropore and mesopore size distributions for the samples are shown in Table 1 and Fig. 2. It can be clearly seen that hydrothermal aging leads to mesopore formation at the expense of micropores due to the partial collapse of the zeolite crystal structure, consistent with the result reported by Gao et al. [8] This would result in facile gas diffusion for the hydrothermally aged samples. Many previous studies have indicated that hydrothermal aging can alter the Cu active sites, form CuO_x clusters, and partially destroy the zeolite structure. [6,7] These changes will definitely influence the NH_3-SCR performance of Cu-SSZ-13 catalysts.

3.2. SSCR and FSCR performance

The NO_x conversion percentages obtained with fresh and hydrothermally aged Cu-SSZ-13 catalysts under standard and fast SCR conditions are shown in Fig. 3. As expected, the NO_x conversion under SSCR conditions decreased with progressive hydrothermal aging due to the loss of active sites and structure degradation. However, it was interestingly observed that under FSCR conditions, the NO_x conversion of hydrothermally aged catalysts was in fact clearly higher than that of the fresh catalyst at low temperatures, and the NO_x conversion of Cu-SSZ-13 increased with the increase of the hydrothermal aging temperature.

We have previously reported that NO_2 addition could inhibit NO_x conversion due to NH_4NO_3 formation, which prevents reactants from diffusing in the micropores. [25,26] Therefore, the formation of mesopores in the hydrothermally aged samples would favor gas diffusion and thereby weaken the inhibition effect of NO_2. In this study, however, the inhibition effect of NO_2 on NO_x conversion was also observed for hydrothermally aged samples, but at much lower temperatures (150 and 175 °C). The difference values between the NO_x conversion percentages under SSCR and FSCR were calculated, and the results are shown in Fig. 4. Significant inhibition of NO_x conversion by NO_2 was observed on the fresh Cu-SSZ-13, while only slight inhibition was observed on Cu-SSZ-13 – 800. When the reaction temperature reached 225 °C, NO_2 even promoted the NO_x conversion of Cu-SSZ-13 – 800. These results clearly indicated that hydrothermal aging could significantly alleviate the inhibition effects of NO_2 on NO_x conversion over Cu-SSZ-13 in the NH_3-SCR reaction.

3.3. NH_3-TPD studies

NH_3-TPD was conducted to investigate the acid sites of fresh and hydrothermally aged Cu-SSZ-13 catalysts. As shown in Fig. 5, two distinct NH_3 desorption peaks were observed for all the three catalysts. The low-temperature peak is ascribed to NH_3 adsorbed on Lewis acid sites (LASs, primarily Cu sites), and the high-temperature peak is due to NH_3 desorbed on Brønsted acid sites (BASs, primarily -Si – OH-Al-) [10,38]. The total amount of NH_3 desorption was calculated, including that from LASs and BASs, and the results are shown in Table 2. Hydrothermal aging induced a progressive loss of total acid sites, from 2.44 mmol/g on Cu-SSZ-13 to 1.40 and 0.75 mmol/g on Cu-SSZ-13 – 750 and Cu-SSZ-13 – 800, respectively. After hydrothermal aging, Cu-SSZ-13 – 750 showed a significant decrease of BASs (from 0.76 to 0.32 mmol/g), which was mainly due to dealumination. On the other hand, most of the active Cu sites were preserved for Cu-SSZ-13 – 750, with relatively high LASs (from 1.68 to 1.08 mmol/g). For the deeply

Table 1
The amounts of Cu species determined by H_2-TPR analysis and micro-and meso-pore volumes of the Cu-SSZ-13, Cu-SSZ-13-750, and Cu-SSZ-13-800 catalysts.

Sample	Cu_{total} (μmol/g)	$Cu(OH)^+$-Z (μmol/g)	Cu^{2+}-2Z (μmol/g)	CuO_x (μmol/g)	Micro-pore volume (cm^3/g)	Meso-pore volume (cm^3/g)	Total pore volume (cm^3/g)
Cu-SSZ-13	569	319	250	0	0.255	0.043	0.298
Cu-SSZ-13 – 750	562	301	226	27	0.224	0.051	0.275
Cu-SSZ-13 – 800	346	127	146	73	0.224	0.052	0.276

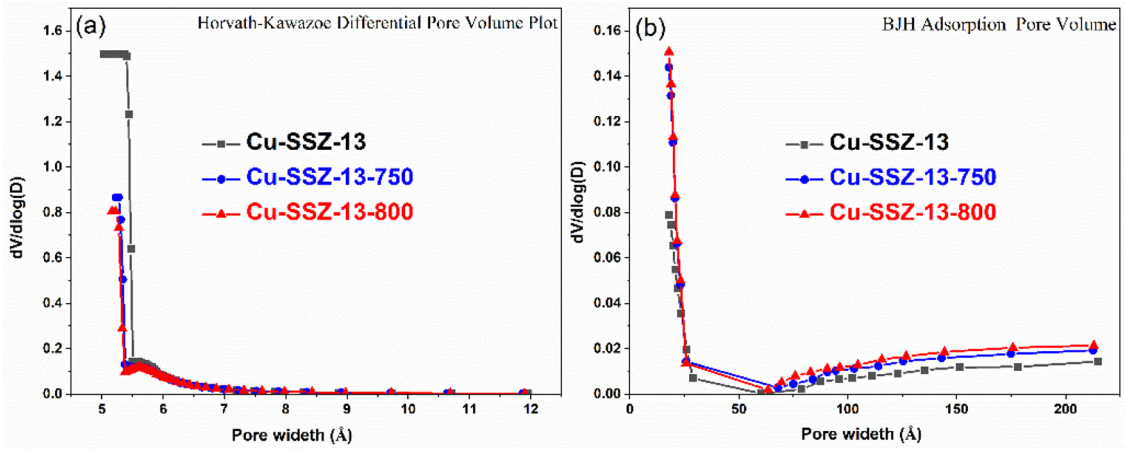

Fig. 2. (a) Micropore size distributions and (b) Mesopore size distributions of fresh and hydrothermally aged Cu-SSZ-13.

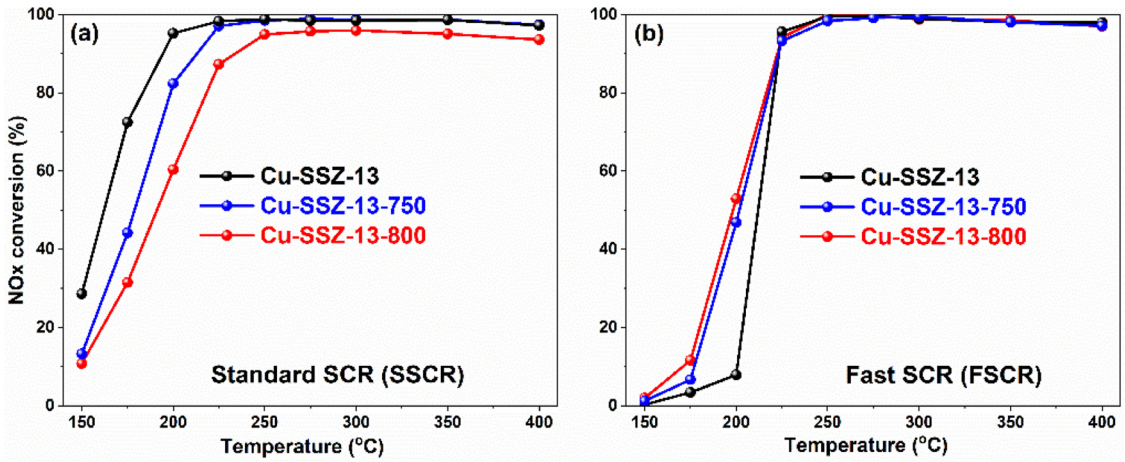

Fig. 3. NH_3-SCR performance of fresh and hydrothermally aged Cu-SSZ-13 catalysts. (a) SSCR conditions: [NO] = [NH_3] = 500 ppm; (b) FSCR conditions: [NO] = [NO_2] = 250 ppm, [NH_3] = 500 ppm. Both 5% O_2 and 5 vol.% H_2O, balance N_2, and GHSV = 400,000 h^{-1}.

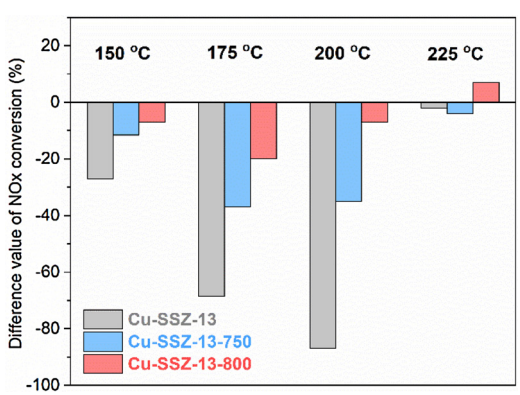

Fig. 4. The difference values between the NO_x conversion percentages under SSCR and FSCR conditions. Difference value of NO_x conversion = NO_x conversion (FSCR) – NO_x conversion (SSCR).

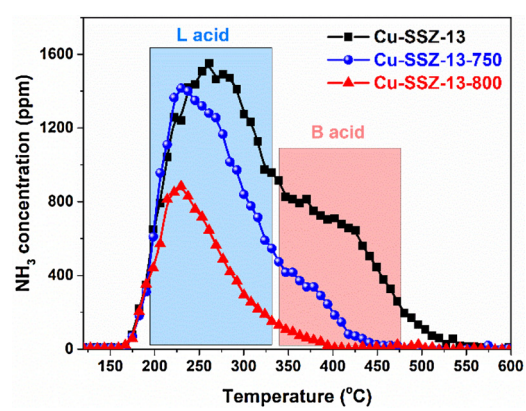

Fig. 5. NH_3-TPD profiles of fresh and hydrothermally aged Cu-SSZ-13 catalysts.

hydrothermally aged Cu-SSZ-13 – 800, the BASs were almost totally lost, with just 0.11 mmol/ g left. Although large amounts of CuO_x clusters formed, the preserved LASs on Cu-SSZ-13 – 800 contributed to its NH_3-SCR performance. Moreover, the desorption temperature of NH_3 for BASs and LASs shifted to the lower temperatures in both cases, indicating a decrease in acid strength after hydrothermal aging. The H_2-TPR results gave the amounts of $Cu(OH)^+$-Z and Cu^{2+}-2Z species, which are coordinated with single Al and paired Al, respectively. The NH_3 desorption from BASs indicated the amounts of uncoordinated Al.

Based on these results, we calculated the coverage of Al with Cu to be 0.52, 0.70 and 0.79 for Cu-SSZ-13, Cu-SSZ-13 – 750 and Cu-SSZ-13 – 800, respectively. The increasing trend of the coverage of Al with Cu indicated that the uncoordinated Al is easily removed, which is in good agreement with our recent finding that Cu^{2+} can protect framework Al from dealumination [12]. The ratio of (non-CuO) Cu to the remaining framework Al is 0.36, 0.49 and 0.52 for Cu-SSZ-13, Cu-SSZ-13 – 750 and Cu-SSZ-13 – 800, respectively.

Table 2
The amounts of desorbed NH_3, NO, and NO_2 in the TPD experiments and NH_4NO_3 accumulation over the Cu-SSZ-13, Cu-SSZ-13-750, and Cu-SSZ-13-800 catalysts.

Sample	NH_3-TPD (mmol/g)			NO-TPD (μmol/g)		NO + O_2-TPD (μmol/g)		NO_2-TPD (μmol/g)		NH_4NO_3 (μmol/g)
	L	B	Total	NO	NO_2	NO	NO_2	NO	NO_2	
Cu-SSZ-13	1.68	0.76	2.44	157	0.00	0.00	66	81	354	779
Cu-SSZ-13 − 750	1.08	0.32	1.40	52	0.00	0.00	40	35	270	43
Cu-SSZ-13 − 800	0.64	0.11	0.75	34	0.00	0.00	23	0	219	7

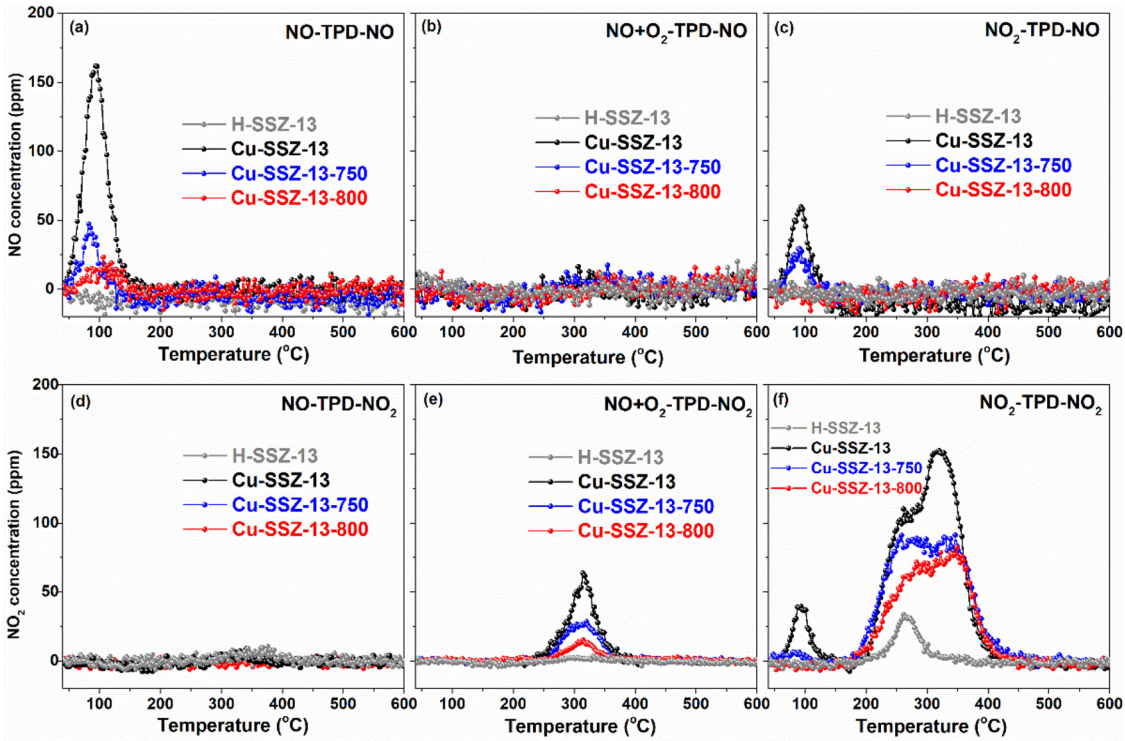

Fig. 6. NO_x-TPD profiles of fresh and hydrothermally aged Cu-SSZ-13 catalysts and H-SSZ-13 zeolite.

3.4. NO_x-TPD studies

NO_x-TPD (NO-TPD, NO + O_2-TPD and NO_2-TPD) was conducted to investigate the adsorbed nitrate species, and the results are shown in Fig. 6. In addition, the desorption amounts of NO and NO_2 were calculated, and the results are shown in Table 2. In the NO-TPD experiment, a NO desorption peak was observed at ~ 100 °C, and no NO_2 desorption was observed. The NO storage decreased from 157 μmol/g for fresh Cu-SSZ-13 to 52 and 34 μmol/g for hydrothermally aged Cu-SSZ-13 − 750 and Cu-SSZ-13 − 800, respectively. This result indicated that NO cannot be oxidized without O_2, but can weakly adsorb on the Cu-SSZ-13 catalyst. As Hammershoi et al. reported in their NO-TPR experiment, NO is consumed by the oxidized Cu formed after heating to 500 in a 5% O_2/N_2 atmosphere. [39] In fact, NO can partially adsorb onto Cu^{2+} active sites to form Cu^{+}-NO^{+} species. [40,41] The observed decrease in NO storage suggested a decrease in Cu^{2+} active sites after hydrothermal aging, which has been also observed in H_2-TPR and NH_3-TPD tests. However, as shown in the NO + O_2-TPD experiment, when O_2 co-existed with NO, no NO desorption was observed, indicating that the Cu^{2+} cannot be reduced by NO in the presence of O_2. Interestingly, a clear peak of NO_2 desorption at about 310 °C was observed for the Cu-SSZ-13 catalysts but not for the H-SSZ-13 zeolite, which indicated that the desorbed NO_2 mainly derived from as nitrate species adsorbed primarily on the Cu sites of the catalysts. This phenomenon is in good agreement with the results reported by Hammershoi et al. that a Cu^{II}-(N,O) phase would form during treatment with NO + O_2 [39]. Based on the NO-TPD and NO + O_2-TPD results, it can be concluded that NO was oxidized by O_2 and then formed nitrate on the Cu^{2+} active sites. The decrease in the amount of NO_2 released (from 66 μmol/g of Cu-SSZ-13 to 40 and 23 μmol/g of Cu-SSZ-13 − 750 and Cu-SSZ-13 − 800, respectively) suggested that hydrothermal aging can weaken the oxidation ability of Cu-SSZ-13.

NO_2-TPD was also carried out, and the results are shown in Fig. 6**c** and **f**. In this test, the desorption of NO was observed again, probably due to the NO_2 disproportionation reaction: [18,42]

$$2NO_2 \rightarrow NO^{+} + NO_3^{-} \quad (3)$$

Compared with NO-TPD, the NO storage in NO_2-TPD was relatively low, probably due to the oxidizing ability of NO_2, which inhibited the reduction of Cu^{2+} by NO. For NO_2 desorption, the Cu-SSZ-13 and Cu-SSZ-13 − 750 catalysts both showed a weak peak at 100 °C, which was ascribed to NO_2 physisorption. The SSZ-13 substrate showed a small peak for NO_2 desorption at ~260 °C, indicating that NO_2 disproportionation could occur on the acid sites to form nitrates and nitrites, which then discomposed with the increase of temperature: [16,21]

$$2NO_2 + Z-OH \leftrightarrow HNO_2 + Z\text{-}NO_3 \quad (4)$$

For the Cu-SSZ-13 catalysts, the main peak of NO_2 desorption was observed at 310 °C where NO_2 desorbed from Cu active sites, which was also observed in the NO + O_2-TPD experiment and a recent study by R. Villamaina et al. [43] Based on an investigation on Cu-SSZ-13 catalysts

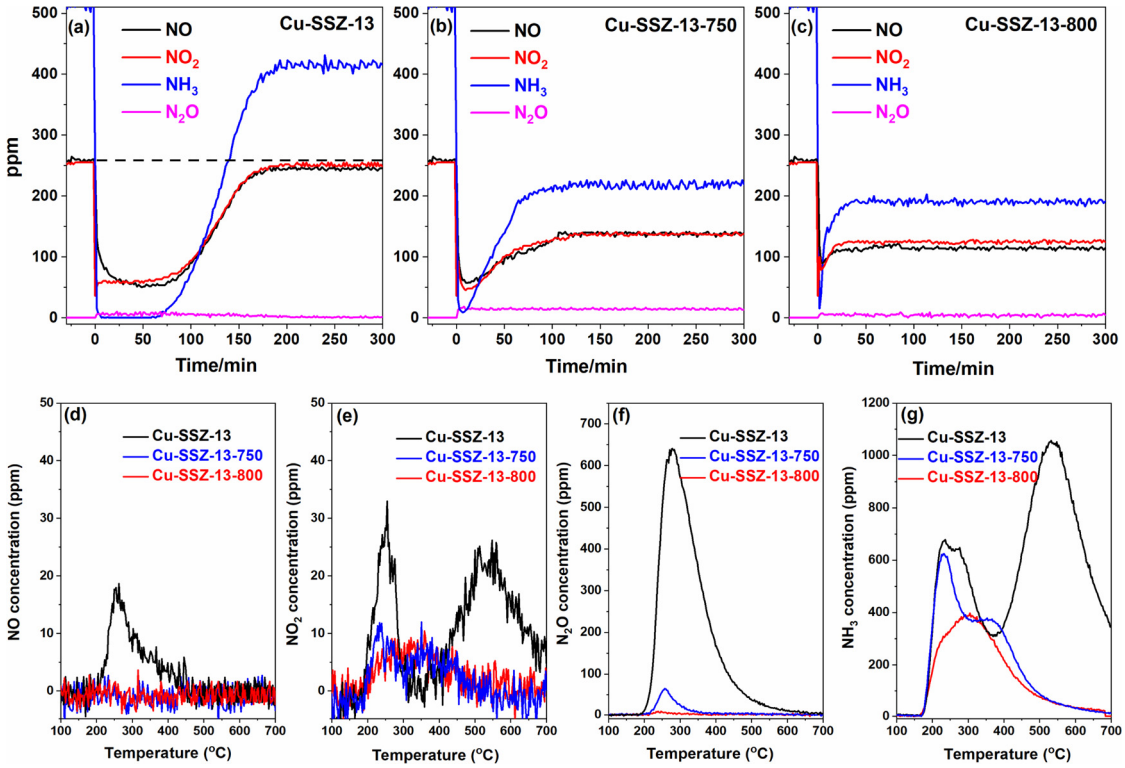

Fig. 7. FSCR-TPD profiles of fresh and hydrothermally aged Cu-SSZ-13. Top profiles are the NO, NO_2, NH_3 and N_2O concentrations during the FSCR reaction of (a) Cu-SSZ-13, (b) Cu-SSZ-13-750 and (c) Cu-SSZ-13-800. Bottom profiles are the (d) NO, (e) NO_2, (f) NH_3 and (g) N_2O concentrations during the TPD process of the three samples after the FSCR reaction.

with different Cu loadings and Si/Al, R. Villamaina et al. proposed that NO_2 only adsorbed onto the $[Cu(OH)]^+$-Z species [43]. By subtracting the NO_2 physisorption, the ratio of NO_2 desorption to $[Cu(OH)]^+$-Z was found to be 1.03 and 0.89 for Cu-SSZ-13 and Cu-SSZ-13 − 750 samples, which is consistent with the results reported by R. Villamaina et al. [43] However, Cu-SSZ-13 − 800 showed a large excess of NO_2, with a NO_2/$[Cu(OH)^+]$ of 1.73, which is desorbed from CuO_x and extra-framework Al.

Therefore, the decrease of NO_2 storage after hydrothermal aging indicated the transformation of $[Cu(OH)]^+$-Z species to Cu^{2+}-2Z species or CuO_x clusters, which has also been confirmed by the H_2-TPR results. The NO_x-TPD results indicated that NO_2 not only forms nitrates on Cu^{2+} active sites, but also can partially adsorb onto the zeolite structure.

3.5. FSCR-TPD studies

The results of the fast SCR reaction over Cu-SSZ-13, Cu-SSZ-13 − 750, and Cu-SSZ-13 − 800 catalysts as a function of time at 200 °C are shown in Fig. 7**a–c**. When the mixed gas flowed through the catalysts, NO, NO_2 and NH_3 first decreased rapidly and then rose gradually for all the three catalysts. Cu-SSZ-13 reached steady-state after reaction for 180 min, and only showed a slight decrease of NO, NO_2 and NH_3 concentrations, indicating the severe inhibiting effect on NO_x conversion due to NH_4NO_3 accumulation. However, Cu-SSZ-13 − 750 and Cu-SSZ-13 − 800 reached steady-state after reaction for only 100 and 30 min, respectively, and the NO_x conversion increased with progressive hydrothermal aging. The time taken to reach steady-state can reflect the amounts of NH_4NO_3 accumulated onto the Cu-SSZ-13 catalysts. Clearly, the accumulation of NH_4NO_3 decreased with progressive hydrothermal aging, which also resulted in a progressive increase in NO_x conversion under FSCR reaction conditions, compared with that under SSCR reaction conditions.

To investigate the species accumulated after the FSCR reaction, a TPD experiment was carried out and the desorption results of NO, NO_2, N_2O and NH_3 are shown in Fig. 7**d–g**. As shown in Fig. 7d, only the fresh Cu-SSZ-13 showed a slight peak of NO desorption, which could be assigned to weakly adsorbed NO. For the NO_2 desorption results in Fig. 7e, the fresh Cu-SSZ-13 sample showed two peaks at ~260 °C and 550 °C, respectively, which are assigned to weakly adsorbed NO_2 on the zeolite framework and possible decomposition of nitrate species [18,44]:

$$4NH_4NO_3 \rightarrow 3N_2 + 2NO_2 + 8H_2O \quad (5)$$

$$4HNO_3 \rightarrow 4NO_2 + 2H_2O + O_2 \quad (6)$$

In fact, the desorbed NO and NO_2 were negligible compared with the desorbed N_2O and NH_3 shown in Fig. 7**f** and **g**. The desorption of N_2O is generally associated with the typical decomposition of NH_4NO_3: [26,45]

$$NH_4NO_3 \rightarrow N_2O + 2H_2O \quad (7)$$

The N_2O outlet concentration decreased with the increase of hydrothermal aging temperature, which indicated that the accumulation of NH_4NO_3 on the hydrothermally aged catalysts was less than that on the fresh catalyst. Moreover, since the NO and NO_2 outlet concentrations were very low, the amount of desorbed N_2O can be used to quantify the accumulated NH_4NO_3 for the catalysts according to the stoichiometry of reaction (7). The storage of NH_4NO_3 on these three catalysts is shown in Table 2. The accumulation of NH_4NO_3 decreased rapidly from 779 for fresh Cu-SSZ-13 to 43 and 7 μmol/g for Cu-SSZ-13 − 750 and Cu-SSZ-13 − 800, respectively, with increasing hydrothermal aging temperature. In addition, the decomposition temperature of NH_4NO_3 shifted from 280 °C to 257 and 246 °C after hydrothermal aging at 750 and 800 °C, respectively, indicating the instability of the formed NH_4NO_3. Therefore, hydrothermal aging decreased the amount of NH_4NO_3 accumulation as well as the stability of NH_4NO_3, which alleviated the inhibition effect on NO_x conversion in the FSCR reaction.

In addition, a large amount of NH_3 was desorbed during the test, as shown in Fig. 7g, which originated from the recovery of acid sites and/or decomposition of ammonium nitrates, which can be expressed as follows: [18]

$$NH_4NO_3 \rightarrow NH_3 + HNO_3 \quad (8)$$

The formed HNO_3 could decompose according to Reaction (6). However, the scant NO_2 desorption observed negated the possibility of significant HNO_3 formation. Therefore, the desorbed NH_3 mainly originated from the Cu^{2+} active sites (LASs) and BASs. As described in the discussion of NH_3-TPD results, the NH_3 desorbed from both Cu^{2+} active sites and BASs decreased with the increase of aging temperature, which is consistent with the CuO_x formation and dealumination that took place during hydrothermal aging, as shown in Fig. 1. The fresh Cu-SSZ-13 catalyst showed a larger NH_3 desorption amount at high temperature compared to that in the NH_3-TPD results (540 °C) due to pore blockage by accumulated ammonia nitrate, which inhibited the NH_3 desorption at low temperatures and preserved more NH_3 for high-temperature desorption. In addition, the NH_3 desorption in this test was lower than that in NH_3-TPD, which can be explained by the fact that some of the absorbed NH_3 reacted with NO_2 to form NH_4NO_3 (decompose to N_2O) or to facilitate the NO_2-SCR reaction. [26,44]

3.6. In situ DRIFTS studies

3.6.1. Steady-state SSCR and FSCR reactions

The adsorbed surface species on the catalysts under steady-state SSCR and FSCR conditions were investigated by *in situ* DRIFTS, and the results are shown in Fig. 8. The negative peaks at 3735 and 3664 cm^{-1} are attributed to the consumption of external Si−OH and Al−OH groups, respectively, due to NH_3 adsorption. The peaks at 3600 and 3570 cm^{-1} are ascribed to the consumption of the strong BASs (Si−OH-Al groups) [14,38]. Concomitantly, the bands due to NH_3 adsorbed on the BASs were observed at 3332, 3273 and 1457 cm^{-1} [46,47]. These peaks decreased progressively with the increase of hydrothermal aging temperature under both the SSCR and FSCR conditions, indicating the loss of BASs due to hydrothermal aging.

Different from the SSCR process, two peaks related to nitrates at 1560 and 1475 cm^{-1} were observed for the FSCR. The band at 1560 cm^{-1} is attributed to copper-nitrate (Cu-NO_3-) and the band at 1475 cm^{-1} is a combination peak of NH_3 species at 1457 cm^{-1} and some nitrate species at ~1500 cm^{-1}. [25,47–49]. Compared with SSCR spectra, the FSCR process showed marked nitrate species accumulation onto the catalysts, regardless of whether they underwent hydrothermal aging or not. Most of these nitrate species coordinated with adsorbed NH_3 species to form NH_4NO_3, which then decomposed at high temperatures, as shown by the FSCR-TPD results. The band at 1620 cm^{-1} was attributed to molecular NH_3 adsorbed on the LASs [47,50]. It was found that the peaks assignable to nitrates were scarcely seen under SSCR conditions at 200 °C, which probably suggested that copper nitrate species are not related to the rate-determining reaction. However, distinct nitrate species peaks were observed under FSCR conditions, which indicated that nitrates are important intermediate species. The peaks at 935 and 900 cm^{-1} are attributed to the zeolite T−O−T vibration perturbed by Cu^{2+} species. [3,51] The decrease of these two peaks after hydrothermal aging indicated the transformation of Cu^{2+} to CuO_x, which we have also observed by H_2-TPR.

3.6.2. Time-resolved SSCR and FSCR reactions

To observe the dynamic changes during the SSCR and FSCR reactions, time-resolved *in situ* DRIFT spectra of the catalysts were obtained and the results are shown in Fig. 9. In the case of the SSCR reaction (Fig. 9**a–c**), IR bands due to NH_3 adsorbed on the LASs (L-NH_3) and BASs (B-NH_3) were observed at 1620 and 1457 cm^{-1}, respectively. It can be seen that B-NH_3 appeared immediately and leveled off, while -L-NH_3 only showed a slight peak at the reaction time of 5 min. After reaction for 20 min, the adsorbed -L-NH_3 on the surface of the three catalysts was saturated. In the case of the FSCR reaction (Fig. 9**d–e**), the peak at 1445 cm^{-1}, which was ascribed to NH_4^+ from NH_4NO_3 as we previously reported [25], appeared immediately when the fast SCR reaction gases were introduced to the catalyst. It can be clearly seen that NH_4NO_3 started to accumulate when the FSCR occurred, and fresh Cu-SSZ-13 accumulated more NH_4NO_3 than hydrothermally aged Cu-SSZ-13 in the first 20 min. From the NO_x- and NH_3-TPD experiments, we found that the NO_2 and NH_3 adsorption amounts decreased with progressive hydrothermal aging. Therefore, the decline of NH_3 and NO_2 adsorption should be responsible for the decrease in NH_4NO_3 formation on the hydrothermally aged catalysts. With time increasing continuously, this peak gradually shifted to higher wavenumbers because NH_3 adsorption on BASs at 1457 cm^{-1}, which was not related to NH_4NO_3, occurred concurrently. This NH_3 adsorption was also identified in Fig. 7g, in which some NH_3 molecules desorbed from BASs. As the reaction proceeds, some nitrate species between 1500−1650 cm^{-1} would accumulate, including some bidentate nitrate at ~1500 cm^{-1} and copper nitrates at 1560 cm^{-1} [47,52,53]. Therefore, the final peak at 1475 cm^{-1} in the steady-state FSCR reaction is a combination peak of ammonia and nitrates.

3.6.3. Transient reaction of adsorbed NH_3 with NO + O_2 and NO_2

The reactions of adsorbed NH_3 with NO + O_2 and NO_2 over Cu-SSZ-

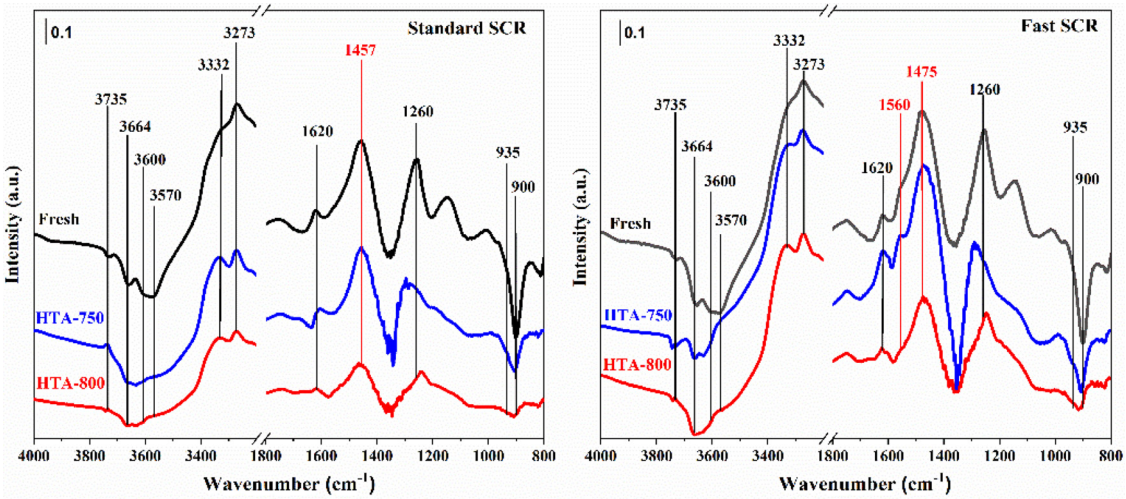

Fig. 8. *In situ* DRIFTS spectra of adsorbed species on Cu-SSZ-13, Cu-SSZ-13-750 and Cu-SSZ-13-800 during the (a) standard SCR and (b) fast SCR reactions.

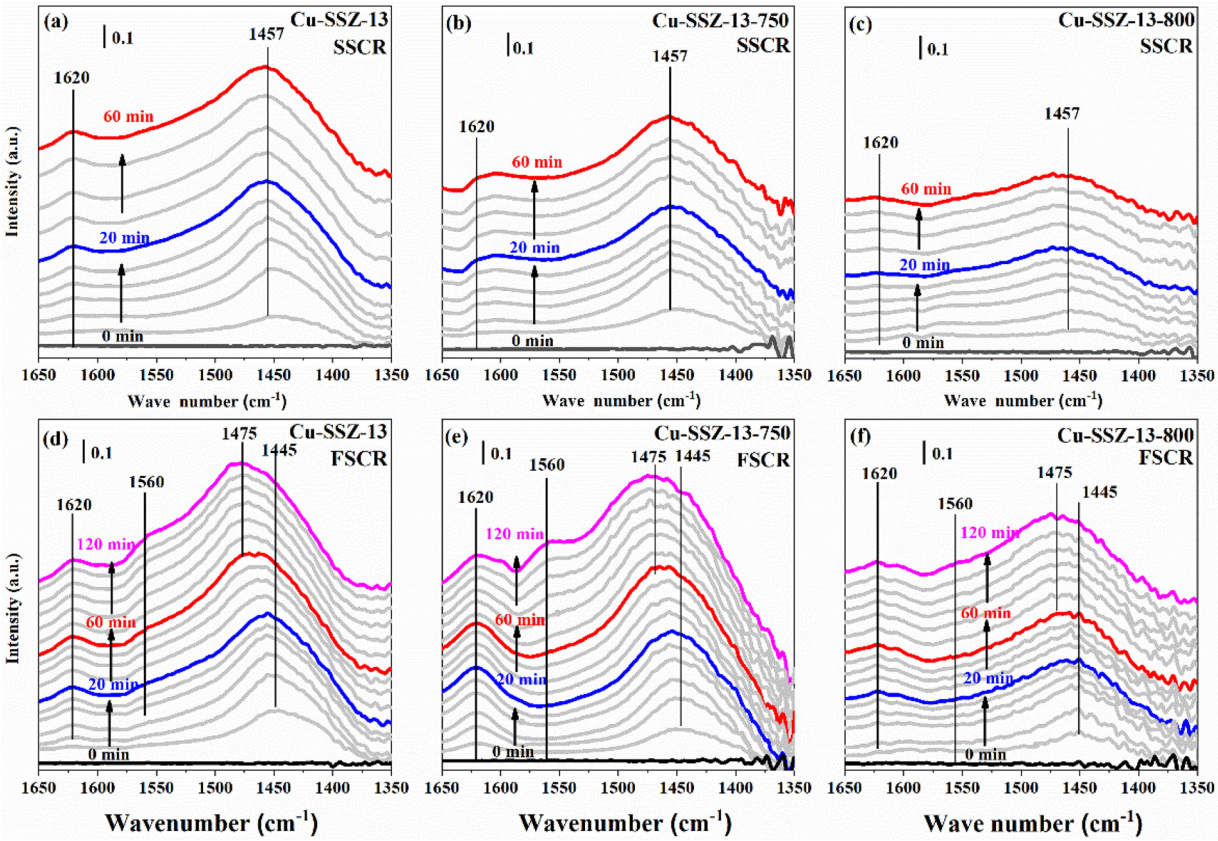

Fig. 9. *In situ* DRIFTS spectra of adsorbed species on (a) Cu-SSZ-13, (b) Cu-SSZ-13-750 and (c) Cu-SSZ-13-800 during the SSCR and (d) Cu-SSZ-13, (e) Cu-SSZ-13-750 and (f) Cu-SSZ-13-800 during the FSCR reaction.

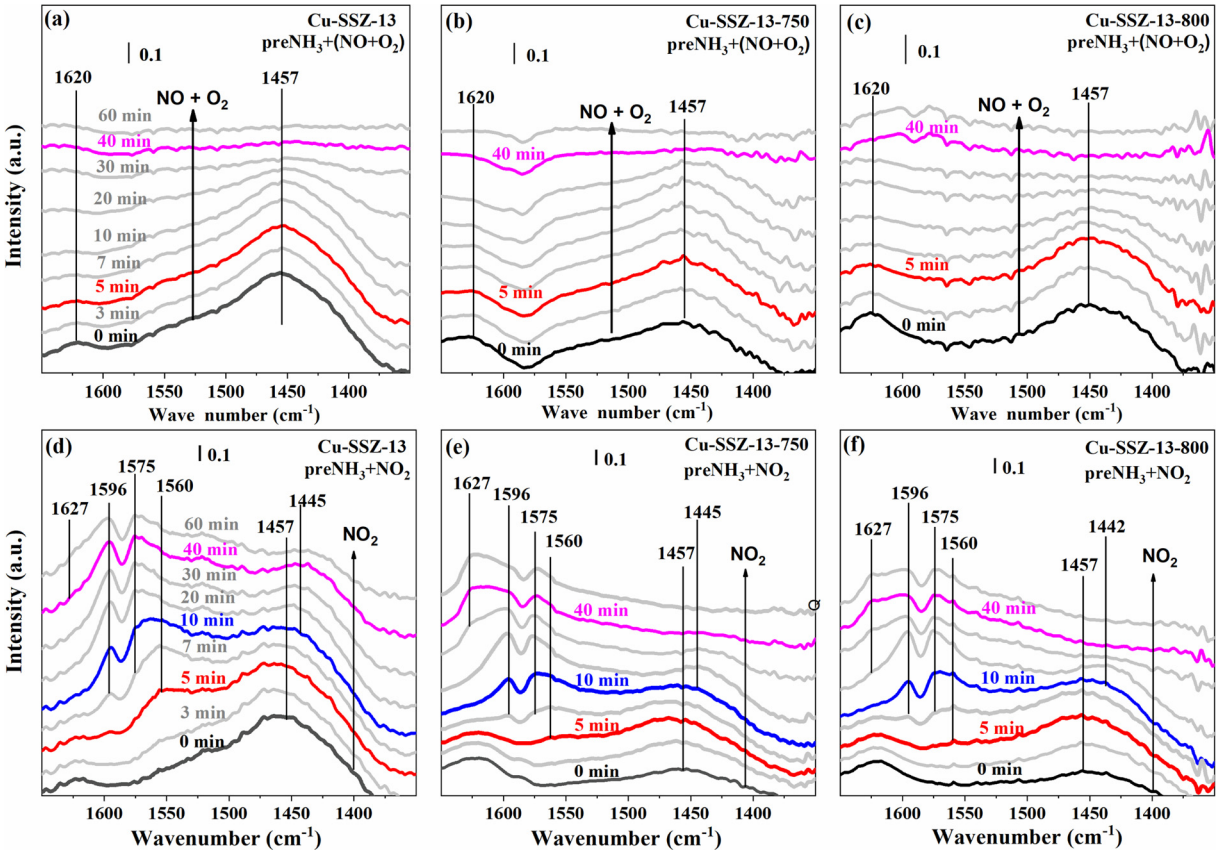

Fig. 10. *In situ* DRIFTS spectra of reaction of adsorbed NH_3 with NO + O_2 (above) and NO_2 (below) over Cu-SSZ-13, Cu-SSZ-13-750 and Cu-SSZ-13-800 catalysts.

13, Cu-SSZ-13 − 750 and Cu-SSZ-13 − 800 catalysts were subsequently investigated, and the results are shown in Fig. 10. Under the flow of NO + O_2, all catalysts showed more active L-NH_3 (1620 cm^{-1}), which immediately reacted with NO + O_2 and almost disappeared at 7 min. Thereafter, B-NH_3 (1457 cm^{-1}) started to be consumed until it disappeared at ~40 min. Therefore, the L-L-NH_3 is more active than B-NH_3 for reaction with NO + O_2, as reported in some other studies. [47,54]

Under the flow of NO_2, it was also observed that -L-NH_3 was consumed first and then B-NH_3, but differently, new peaks representing nitrates appeared between 1500 and 1700 cm^{-1} with the consumption of B-NH_3. After reaction for 5 min, a typical peak assigned to NH_4NO_3 (1445 cm^{-1}) appeared accompanied with the consumption of B-NH_3. This result indicated that B-NH_3 is primarily responsible for the formation of NH_4NO_3, while -L-NH_3 is more active for reaction with NO_2 to form N_2. In addition, the peak attributed to NH_4NO_3 remained for fresh Cu-SSZ-13 after reaction for 60 min, while this peak almost disappeared for both Cu-SSZ-13 − 750 and Cu-SSZ-13 − 800. This result indicated that the consumption of NH_4NO_3 on fresh Cu-SSZ-13 is more difficult than that on aged catalysts *via* reaction (7) or reduction by NO (reaction (9)):

$$NH_4NO_3 + NO \rightarrow N_2 + NO_2 + 2H_2O \quad (9)$$

After adsorbed NH_3 was fully consumed, a large amount of nitrates (1500 − 1700 cm^{-1}) was observed under the NO_2 atmosphere, which is significantly different from the conditions of NO + O_2.

4. Conclusions

Taking all the above results into account, the adsorption capacity of NH_3 on BASs is important for the formation of NH_4NO_3, while -L-NH_3 is more reactive in both NO + O_2 and NO_2 for the formation of N_2. Hydrothermal aging resulted in a decrease in the amount of BASs as well as the NH_3 adsorption strength, further alleviating the accumulation of NH_4NO_3 during the FSCR reaction. The amount and decomposition temperature of accumulated NH_4NO_3 both significantly decreased with progressive hydrothermal aging. Moreover, the formation of mesopores induced by hydrothermal aging is favorable for gas diffusion. As a result, the inhibition effect of NO_2 on NO_x conversion was weakened for the hydrothermally aged Cu-SSZ-13 catalysts. The results presented in this work have great significance for the actual application of diesel emission control, especially under fast SCR conditions.

CRediT authorship contribution statement

Yulong Shan: Formal analysis, Investigation, Writing - original draft, Writing - review & editing, Funding acquisition. **Yu Sun:** Investigation, Data curation. **Jinpeng Du:** Investigation, Data curation. **Yan Zhang:** Investigation, Data curation. **Xiaoyan Shi:** Supervision, Funding acquisition. **Yunbo Yu:** Resources, Supervision. **Wenpo Shan:** Supervision, Writing - review & editing, Project administration, Funding acquisition. **Hong He:** Resources, Supervision, Funding acquisition.

Declaration of Competing Interest

The authors declare that they have no known competing financial interests or personal relationships that could have appeared to influence the work reported in this paper.

Acknowledgments

This work was financially supported by the National Natural Science Foundation of China (21637005, 51822811, 21906172, 51978640)

Appendix A. Supplementary data

Supplementary material related to this article can be found, in the online version, at doi:https://doi.org/10.1016/j.apcatb.2020.119105.

References

[1] R. Zhang, N. Liu, Z. Lei, B. Chen, Selective transformation of various nitrogen-containing exhaust gases toward N_2 over zeolite catalysts, Chem. Rev. 116 (2016) 3658–3721.
[2] J.H. Kwak, D. Tran, S.D. Burton, J. Szanyi, J.H. Lee, C.H.F. Peden, Effects of hydrothermal aging on NH_3-SCR reaction over Cu/zeolites, J. Catal. 287 (2012) 203–209.
[3] J. Luo, D. Wang, A. Kumar, J. Li, K. Kamasamudram, N. Currier, A. Yezerets, Identification of two types of Cu sites in Cu/SSZ-13 and their unique responses to hydrothermal aging and sulfur poisoning, Catal. Today 267 (2016) 3–9.
[4] S.J. Schmieg, S.H. Oh, C.H. Kim, D.B. Brown, J.H. Lee, C.H.F. Peden, D.H. Kim, Thermal durability of Cu-CHA NH_3-SCR catalysts for diesel NO_x reduction, Catal. Today 184 (2012) 252–261.
[5] Y.J. Kim, J.K. Lee, K.M. Min, S.B. Hong, I.-S. Nam, B.K. Cho, Hydrothermal stability of CuSSZ13 for reducing NO_x by NH_3, J. Catal. 311 (2014) 447–457.
[6] S. Han, J. Cheng, C. Zheng, Q. Ye, S. Cheng, T. Kang, H. Dai, Effect of Si/Al ratio on catalytic performance of hydrothermally aged Cu-SSZ-13 for the NH_3-SCR of NO in simulated diesel exhaust, Appl. Sur. Sci. 419 (2017) 382–392.
[7] S. Han, Q. Ye, S. Cheng, T. Kang, H. Dai, Effect of the hydrothermal aging temperature and Cu/Al ratio on the hydrothermal stability of CuSSZ-13 catalysts for NH_3-SCR, Catal. Sci. Technol. 7 (2017) 703–717.
[8] J. Song, Y. Wang, E.D. Walter, N.M. Washton, D. Mei, L. Kovarik, M.H. Engelhard, S. Prodinger, Y. Wang, C.H.F. Peden, F. Gao, Toward rational design of Cu/SSZ-13 selective catalytic reduction catalysts: implications from atomic-level understanding of hydrothermal stability, ACS Catal. 7 (2017) 8214–8227.
[9] F. Gao, J. Szanyi, On the hydrothermal stability of Cu/SSZ-13 SCR catalysts, Appl. Catal. A Gen. 560 (2018) 185–194.
[10] J. Luo, F. Gao, K. Kamasamudram, N. Currier, C.H.F. Peden, A. Yezerets, New insights into Cu/SSZ-13 SCR catalyst acidity. Part I: Nature of acidic sites probed by NH_3 titration, J. Catal. 348 (2017) 291–299.
[11] L. Ma, Y. Cheng, G. Cavataio, R.W. McCabe, L. Fu, J. Li, Characterization of commercial Cu-SSZ-13 and Cu-SAPO-34 catalysts with hydrothermal treatment for NH_3-SCR of NO_x in diesel exhaust, Chem. Eng. J. 225 (2013) 323–330.
[12] Y. Shan, J. Du, Y. Yu, W. Shan, X. Shi, H. He, Precise control of post-treatment significantly increases hydrothermal stability of in-situ synthesized cu-zeolites for NH_3-SCR reaction, Appl. Catal. B 266 (2020) 118655.
[13] X. Ye, J. Schmidt, R.-P. Wang, I. van Ravenhorst, R. Oord, T. Chen, F. de Groot, F. Meirer, B.M. Weckhuysen, Deactivation of Cu-exchanged automotive emissions NH_3-SCR catalysts elucidated with nanoscale resolution using scanning transmission X-ray microscopy, Angew. Chem. Int. Ed. (2020), https://doi.org/10.1002/ange.201916554.
[14] Y. Shan, X. Shi, Z. Yan, J. Liu, Y. Yu, H. He, Deactivation of Cu-SSZ-13 in the presence of SO_2 during hydrothermal aging, Catal. Today 320 (2019) 84–90.
[15] L. Wei, D. Yao, F. Wu, B. Liu, X. Hu, X. Li, X. Wang, Impact of hydrothermal aging on SO_2 poisoning over Cu-SSZ-13 diesel exhaust SCR catalysts, Ind. Eng. Chem. Res. 58 (2019) 3949–3958.
[16] M. Iwasaki, H. Shinjoh, A comparative study of "standard", "fast" and "NO_2" SCR reactions over Fe/zeolite catalyst, Appl. Catal. A Gen. 390 (2010) 71–77.
[17] O. Mihai, C. Widyastuti, A. Kumar, J. Li, S. Joshi, K. Kamasamudram, N. Currier, A. Yezerets, L. Olsson, The effect of NO_2/NO_x feed ratio on the NH_3-SCR system over Cu–zeolites with varying copper loading, Catal. Lett. 144 (2014) 70–80.
[18] H.-Y. Chen, Z. Wei, M. Kollar, F. Gao, Y. Wang, J. Szanyi, C.H.F. Peden, A comparative study of N_2O formation during the selective catalytic reduction of NO_x with NH_3 on zeolite supported Cu catalysts, J. Catal. 329 (2015) 490–498.
[19] H. Sjövall, R.J. Blint, L. Olsson, Detailed kinetic modeling of NH_3-SCR over Cu-ZSM-5, Appl. Catal. B 92 (2009) 138–153.
[20] T.V.W. Janssens, H. Falsig, L.F. Lundegaard, P.N.R. Vennestrøm, S.B. Rasmussen, P.G. Moses, F. Giordanino, E. Borfecchia, K.A. Lomachenko, C. Lamberti, S. Bordiga, A. Godiksen, S. Mossin, P. Beato, A consistent reaction scheme for the selective catalytic reduction of nitrogen oxides with ammonia, ACS Catal. 5 (2015) 2832–2845.
[21] A. Grossale, I. Nova, E. Tronconi, D. Chatterjee, M. Weibel, NH_3–NO/NO_2 SCR for diesel exhausts aftertreatment: Reactivity, mechanism and kinetic modelling of commercial Fe- and Cu-promoted zeolite catalysts, Top. Catal. 52 (2009) 1837–1841.
[22] X. Wang, A. Shi, Y. Duan, J. Wang, M. Shen, Catalytic performance and hydrothermal durability of CeO_2–V_2O_5–ZrO_2/WO_3–TiO_2 based NH_3-SCR catalysts, Catal. Sci. Technol. 2 (2012) 1386–1395.
[23] X. Shi, F. Liu, L. Xie, W. Shan, H. He, NH_3-SCR performance of fresh and hydrothermally aged Fe-ZSM-5 in standard and fast selective catalytic reduction reactions, Environ. Sci. Technol. 47 (2013) 3293–3298.
[24] J.H. Kwak, D. Tran, J. Szanyi, C.H.F. Peden, J.H. Lee, The effect of copper loading on the selective catalytic reduction of nitric oxide by ammonia over Cu-SSZ-13, Catal. Lett. 142 (2012) 295–301.
[25] L. Xie, F. Liu, K. Liu, X. Shi, H. He, Inhibitory effect of NO_2 on the selective catalytic reduction of NO_x with NH_3 over one-pot-synthesized Cu–SSZ-13 catalyst, Catal. Sci. Technol. 4 (2014) 1104–1110.
[26] Y. Shan, X. Shi, G. He, K. Liu, Z. Yan, Y. Yu, H. He, Effects of NO_2 addition on the

NH_3-SCR over small-pore Cu–SSZ-13 zeolites with varying cu loadings, J. Phy. Chem. C 122 (2018) 25948–25953.
[27] L. Ren, L. Zhu, C. Yang, Y. Chen, Q. Sun, H. Zhang, C. Li, F. Nawaz, X. Meng, F.S. Xiao, Designed copper-amine complex as an efficient template for one-pot synthesis of Cu-SSZ-13 zeolite with excellent activity for selective catalytic reduction of NO_x by NH_3, Chem. Commun. 47 (2011) 9789–9791.
[28] J. Hun Kwak, H. Zhu, J.H. Lee, C.H. Peden, J. Szanyi, Two different cationic positions in Cu-SSZ-13? Chem. Commun. 48 (2012) 4758–4760.
[29] C.W. Andersen, M. Bremholm, P.N. Vennestrom, A.B. Blichfeld, L.F. Lundegaard, B.B. Iversen, Location of Cu^{2+} in CHA zeolite investigated by X-ray diffraction using the Rietveld/maximum entropy method, IUCrJ 1 (2014) 382–386.
[30] Y. Jangjou, Q. Do, Y. Gu, L.-G. Lim, H. Sun, D. Wang, A. Kumar, J. Li, L.C. Grabow, W.S. Epling, Nature of Cu active centers in Cu-SSZ-13 and their responses to SO_2 exposure, ACS Catal. 8 (2018) 1325–1337.
[31] F. Gao, E.D. Walter, E.M. Karp, J. Luo, R.G. Tonkyn, J.H. Kwak, J. Szanyi, C.H.F. Peden, Structure–activity relationships in NH_3-SCR over Cu-SSZ-13 as probed by reaction kinetics and EPR studies, J. Catal. 300 (2013) 20–29.
[32] L. Xie, F. Liu, X. Shi, F.-S. Xiao, H. He, Effects of post-treatment method and Na co-cation on the hydrothermal stability of Cu–SSZ-13 catalyst for the selective catalytic reduction of NO_x with NH_3, Appl. Catal. B 179 (2015) 206–212.
[33] J.H. Kwak, R. Tonkyn, D. Tran, D. Mei, S.J. Cho, L. Kovarik, J.H. Lee, C.H.F. Peden, J. Szanyi, Size-dependent catalytic performance of CuO on γ-Al_2O_3: NO reduction versus NH_3 oxidation, ACS Catal. 2 (2012) 1432–1440.
[34] K. Leistner, L. Olsson, Deactivation of Cu/SAPO-34 during low-temperature NH_3-SCR, Appl. Catal. B 165 (2015) 192–199.
[35] J. Du, X. Shi, Y. Shan, Y. Wang, W. Zhang, Y. Yu, W. Shan, H. He, The effect of crystallite size on low-temperature hydrothermal stability of Cu-SAPO-34, Catal. Sci. Technol. (2020), https://doi.org/10.1039/d0cy00414f.
[36] M. Haouas, F. Taulelle, C. Martineau, Recent advances in application of ^{27}Al NMR spectroscopy to materials science, Prog. Nucl. Magn. Reson. Spectrosc. 94-95 (2016) 11–36.
[37] S. Prodinger, M.A. Derewinski, Y. Wang, N.M. Washton, E.D. Walter, J. Szanyi, F. Gao, Y. Wang, C.H.F. Peden, Sub-micron Cu/SSZ-13: synthesis and application as selective catalytic reduction (SCR) catalysts, Appl. Catal. B 201 (2017) 461–469.
[38] D. Wang, F. Gao, C.H.F. Peden, J. Li, K. Kamasamudram, W.S. Epling, Selective catalytic reduction of NO_x with NH_3 over a Cu-SSZ-13 catalyst prepared by a solid-state ion-exchange method, Chem. Commun. 6 (2014) 1579–1583.
[39] P.S. Hammershøi, C. Negri, G. Berlier, S. Bordiga, P. Beato, T.V.W. Janssens, Temperature-programmed reduction with NO as a characterization of active Cu in Cu-CHA catalysts for NH_3-SCR, Catal. Sci. Technol. 9 (2019) 2608–2619.
[40] R. Zhang, J.-S. McEwen, M. Kollár, F. Gao, Y. Wang, J. Szanyi, C.H.F. Peden, NO chemisorption on Cu/SSZ-13: a comparative study from infrared spectroscopy and DFT calculations, ACS Catal. 4 (2014) 4093–4105.
[41] J.H. Kwak, J.H. Lee, S.D. Burton, A.S. Lipton, C.H. Peden, J. Szanyi, A common intermediate for N_2 formation in enzymes and zeolites: side-on Cu-nitrosyl complexes, Angew. Chem. Int. Ed. 125 (2013) 10169–10173.
[42] M.P. Ruggeri, I. Nova, E. Tronconi, J.E. Collier, A.P.E. York, Structure-activity relationship of different Cu-zeolite catalysts for NH_3-SCR, Top. Catal. 59 (2016) 875–881.
[43] R. Villamaina, S. Liu, I. Nova, E. Tronconi, M.P. Ruggeri, J. Collier, A. York, D. Thompsett, Speciation of Cu cations in Cu-CHA catalysts for NH_3-SCR: Effects of SiO_2/Al_2O_3 ratio and Cu-loading investigated by transient response methods, ACS Catal. 9 (2019) 8916–8927.
[44] A. Wang, P. Arora, D. Bernin, A. Kumar, K. Kamasamudram, L. Olsson, Investigation of the robust hydrothermal stability of Cu/LTA for NH_3-SCR reaction, Appl. Catal. B 246 (2019) 242–253.
[45] A. Grossale, I. Nova, E. Tronconi, Ammonia blocking of the "Fast SCR" reactivity over a commercial Fe-zeolite catalyst for Diesel exhaust aftertreatment, J. Catal. 265 (2009) 141–147.
[46] L. Ma, Y. Cheng, G. Cavataio, R.W. McCabe, L. Fu, J. Li, In situ DRIFTS and temperature-programmed technology study on NH_3-SCR of NO_x over Cu-SSZ-13 and Cu-SAPO-34 catalysts, Appl. Catal. B 156-157 (2014) 428–437.
[47] Y. Zhang, Y. Peng, K. Li, S. Liu, J. Chen, J. Li, F. Gao, C.H.F. Peden, Using transient FTIR spectroscopy to probe active sites and reaction intermediates for selective catalytic reduction of NO on Cu/SSZ-13 catalysts, ACS Catal. 6 (2019) 6137–6145.
[48] K.I. Hadjiivanov, Identification of neutral and charged N_xO_y surface species by IR spectroscopy, Catal. Rev. 42 (2000) 71–144.
[49] F. Liu, H. He, Selective catalytic reduction of NO with NH_3 over manganese substituted iron titanate catalyst: reaction mechanism and H_2O/SO_2 inhibition mechanism study, Catal. Today 153 (2010) 70–76.
[50] Y. Shan, X. Shi, J. Du, Y. Yu, H. He, Cu-exchanged RTH-type zeolites for NH_3-selective catalytic reduction of NO_x: Cu distribution and hydrothermal stability, Catal. Sci. Technol. 9 (2019) 106–115.
[51] Y. Ma, S. Cheng, X. Wu, Y. Shi, L. Cao, L. Liu, R. Ran, Z. Si, J. Liu, D. Weng, Low-temperature solid-state ion-exchange method for preparing Cu-SSZ-13 selective catalytic reduction catalyst, ACS Catal. 9 (2019) 6962–6973.
[52] H. Kubota, C. Liu, T. Toyao, Z. Maeno, M. Ogura, N. Nakazawa, S. Inagaki, Y. Kubota, K.-i. Shimizu, Formation and reactions of NH_4NO_3 during transient and steady-state NH_3-SCR of NO_x over H-AFX zeolites: spectroscopic and theoretical studies, ACS Catal. 10 (2020) 2334–2344.
[53] D. Meng, Q. Xu, Y. Jiao, Y. Guo, Y. Guo, L. Wang, G. Lu, W. Zhan, Spinel structured $Co_aMn_bO_x$ mixed oxide catalyst for the selective catalytic reduction of NO_x with NH_3, Appl. Catal. B 221 (2018) 652–663.
[54] H. Zhu, J.H. Kwak, C.H.F. Peden, J. Szanyi, In situ DRIFTS-MS studies on the oxidation of adsorbed NH_3 by NO_x over a Cu-SSZ-13 zeolite, Catal. Today 205 (2013) 16–23.